AN AMPUTATION SIMULATOR WITH BONE SAWING HAPTIC INTERACTION

MING-SHIUM HSIEH[1], MING-DAR TSAI[2], YI-DER YEH[3]

[1]Department of Orthopaedics and Traumatology, Taipei Medical University Hospital, Taipei Medical University, Taipei,
[2]Institute of Information and Computer Engineering, Chung Yuan Christian University, Chung Li,
[3]Department of information and Electornic Commerce, Kainan University, Taoyuan, Taiwan

ABSTRACT

This paper describes a haptic device equipped surgical simulator that provides visual and haptic responses for amputation surgery. This simulator, based on our reported volume (constituted from CT slices) manipulation algorithms, can compute and demonstrate bone changes for the procedures in various orthopedic surgeries. The system is equipped with a haptic device. The position and attitude the haptic device are transformed into the volume to simulate and render the oscillating virtual saw together with the virtual bones. The system then judges if every saw tooth immersing in (cutting) any bone. The load for removing the bone chip on a cutting tooth is calculated according to the feed rate, oscillating speed, saw geometry and bone type. The loads on all the saw teeth are then summed into the three positional forces that the haptic device generates and thus the user feels. The system provides real-time visual and haptic refresh speeds for the sawing procedures. A simulation example of amputation surgery demonstrates the sawing haptic and visual feelings of the sawing procedure are consistent and the simulated sawing force resembles the real force. Therefore, this prototype simulator demonstrates the effectiveness as a surgical simulator to rehearsal the surgical procedures, confirm surgical plains and train interns and students.

Biomed Eng Appl Basis Comm, 2006(October); 18: 229-236.
Keywords: 3D image reconstruction and surgical simulation; sawing force computation; amputation surgery; haptic interaction

1. INTRODUCTION

Recently, many simulation systems have been developed to provide visual confirming and rehearing for surgical modalities in different surgical fields such as orthopedic [1-6], maxillofacial [7-9] and laparoscopic [10-14] surgeries. Meanwhile, haptic feedback is also considered as necessary in several surgical fields and has been implemented in some surgical simulator such as cutting deformable organs [10-14], and burring the skull [15] and teeth [16].

Bone sawing procedures carve out bone shape in ostectomy, osteotomy, artroplasty and amputation surgery. Stable sawing brings good cutting surfaces that are necessary for healing after amputation surgery. However, bone sawing resistance is usually large and change abruptly to result in unstable sawing; therefore, the sawing procedures require a high level of dexterity and experience [17]. Sawing on synthetic bones or real bones (obtained from sectioned frozen bones) is the

Received: June 22, 2006; Accepted: August 18, 2006
Correspondence: Ming-Dar Tsai, Professor and Chairman
Institute of Information and Computer Engineering, Chung Yuan Christian University, Chung Li, 32023 Taiwan
E-mail: tsai@ ice.cycu.edu.tw

current primary training method [17]. However, training of sawing on a virtual patient with complex bone geometric changes as sawing on real human is required [18]. Therefore, a computer simulator for the amputation surgery is expected to demonstrate all geometric changes and provide haptic bone sawing feeling.

This paper introduces a computer system for amputation surgery that adds the sawing haptic functions on our reported orthopedic simulator [19]. This simulator manipulate volume data (constituted from parallel tomographic, such as CT or MRI slice) to recognize new separate bones carved out from saw-swept surfaces and then to delete, reposition and fuse separate bones. These haptic functions represent force responses when using a saw to touch or saw a bone. The system uses a haptic device with 6D (three positions and three angles) input data to simulate the saw position and attitude and to calculate whether the saw touches or immerses into any bone. The (volume manipulated) geometric information about bone touching and immersing is then used to calculate the touch resistance and the sawing force for 3D-rendering the haptic device (letting the device generate 3 forces along the three primary axes of the haptic device). The effectiveness of the simulator was evaluated by simulating an amputation surgery from CT transverse sections of a knee amputation patient.

2. SUBJECT AND METHODS

2.1 System Structure

Figure 1 shows the system architecture. A haptic device with 6D input and 3D output abilities is attached to the system to provide the tactile environment. The input 6D information of the haptic device together with the saw data are used to calculate the saw position, attitude and speed as described in Section 2.2. The saw position, attitude and speed data together with the patient volume data are used to compute the saw touch resistance (described in Section 2.3) and cutting forces (described in Section 2.4). The touch resistance is used to prevent the saw penetration into bones when it is not in sawing (oscillating).

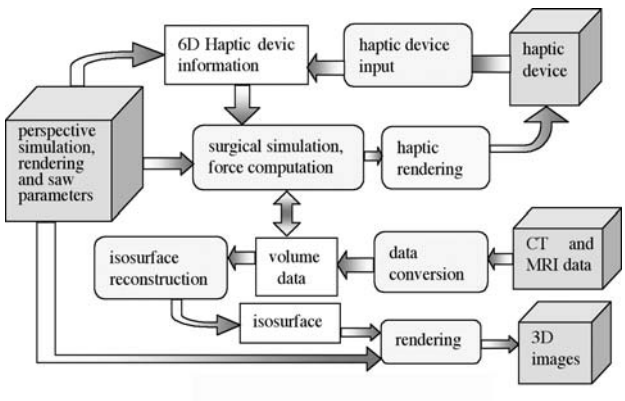

Fig. 1. System architecture.

The patient volume is converted as the data structure that the prototype system can manipulate [19]. The isosurfaces for any specific tissue or structure is generated using the marching cubes algorithm [20]. The triangulated isosurfaces and the dynamic saw are then rendered through the OpenGL libraries. When changing the perspective, the isosurface reconstruction is not required, thus real-time re-rendering can be achieved. Currently, the simulations for orthopedic procedures such as osteotomy, ostectomy, and bone reposition and fusion can achieve interactive responses because isosurface reconstruction is involved. Therefore, the patient volume is not refreshed during the sawing process to achieve real-time re-rendering for the saw oscillation and the new position. The isosurface reconstruction for the sawing process is implemented after the sawed bone is judged to separate to remove.

Currently, the system is implemented on a dual CPU P-IV 3.0G with the graphics card of QUADRO4_980_XGL (by NVIDIA Inc.) to achieve the real-time haptic rendering (over 1000 HZ) and the saw rendering (over 30HZ). The system uses the Phantom Desktop haptic device (by Sensable Inc.) that can provide 3D positional forces and 6D positional sensing more than 1100 dpi resolution. Therefore, real-time visual and smooth haptic responses for the amputation surgery can be achieved with our prototype system.

2.2 Saw Position, Attitude and Speed Computation

The pen-like haptic device attached with a saw (as illustrated in Fig. 2(A)) is used to simulate a real saw attached hand-piece (Fig. 2(B)). The saw attitude, the q-axis of the saw coordinate system is set as perpendicular to the haptic device attitude, the x-axis of the haptic device coordinate system. Therefore, the q-axis coincides to the z-axis of the haptic device coordinate system as illustrated in Fig. 2(C). The s-axis and t-axis are the other two saw primary axes, parallel to the x-axis and y-axis of the haptic device coordinate system, respectively. The saw oscillates about the t-axis (the qs-plane). The haptic device primary axes, the x-axis, y-axis and z-axis are three directions the calculated touch resistance and sawing force act along.

The difference of the two vectors q and q' (the attitude of the previous instant) becomes the rotation of the device attitude and the difference of the device

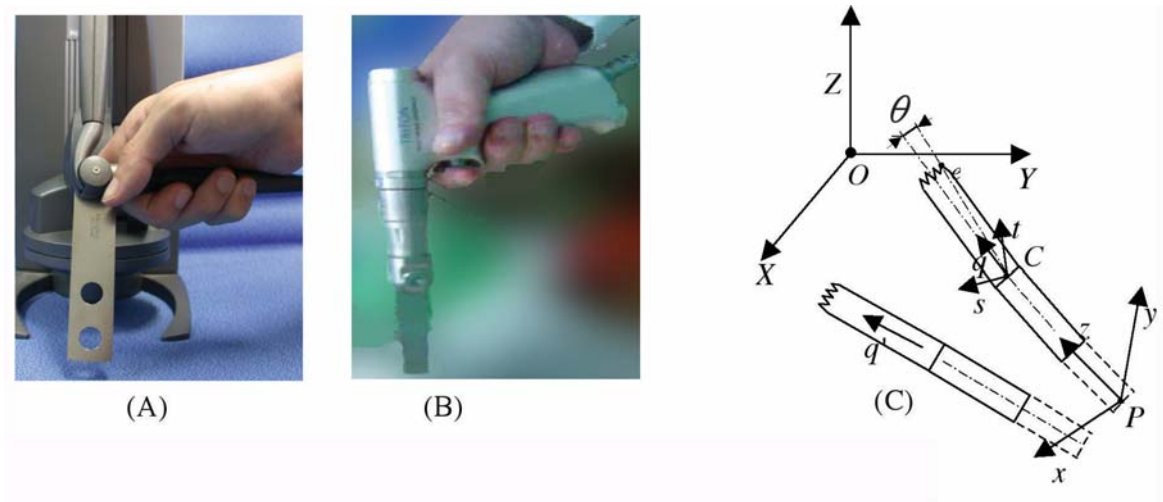

Fig.2. Position and attitude calculation for virtual saw attached hand-piece.
(A) Haptic device for simulating saw attached hand-piece.
(B) Real saw attached hand-piece.
(C) Saw attitude and position determination using 6D data of haptic point.
P, C, O : origins of haptic device, saw coordinate system and volume coordinate system

positions P and P' becomes the device translation. These rotation and translation dividing the haptic sample frequency determine the device linear v and rotational ω velocities (at P). The component of v along the z-axis (or q-axis) is defined as the feed speed, f. The device position and the velocities are then used to calculate the position and the linear velocity at every point of the saw. For example, the position and velocity at the saw origin C is equal to $l\begin{bmatrix}0\\0\\1\end{bmatrix}$ and $v\text{-}\omega \times l\begin{bmatrix}0\\0\\1\end{bmatrix}$, respectively. l, the saw length, is the distance from the saw origin to the saw tip. The position of any saw tooth (as e in Fig. 2(C)) is calculated as $l\begin{bmatrix}0\\0\\1\end{bmatrix}+\begin{bmatrix}0\\0\\r\end{bmatrix}$ $\begin{bmatrix}\cos(\theta) & 0 & \sin(\theta)\\ 0 & 1 & 0\\ -\sin(\theta) & 0 & \cos(\theta)\end{bmatrix}$. r the distance from the saw origin to the saw tooth depends on the tooth position and the saw type. θ, the angle of this tooth on the qs-plane, is equal to $\beta+\alpha$. β, the angular position of the tooth about the saw axis (Fig.2(C)), is equal to $\tan^{-1}\left(\frac{l}{np-c(np)^2}\right).p$, the saw tooth pitch is the distance between two teeth. c represents the effect of the saw geometry. It is 0 if the saw tooth tips form a line. n is the number of teeth from the saw axis to the point. α, the oscillating angle of the saw axis, is determined from the oscillating frequency and amplitude.

The above haptic device coordinate (in real size) can be transformed to the volume coordinate (in voxel size) through the following concatenating affine transformations.

$$\begin{bmatrix}X\\Y\\Z\end{bmatrix} = S_{XZ}S_Y\,TR\begin{bmatrix}x\\y\\z\end{bmatrix}$$

The scaling S_{XZ}, corresponds to the inverse of the voxel width (FOV) and is uniform for all tomographic slices that constitute the volume. The scaling S_Y equals to inverse of the slice thickness. The translation, T means the distance from the haptic device origin to the volume coordinate system origin. The rotation R, corresponds to the angle between the volume and the haptic device coordinate systems and is constituted by three primary haptic device (x, y and z axis) axes represented in the volume coordinate. Similarly, the volume coordinate can be transformed to the haptic device coordinate through the inversions of the above transformations.

2.3 Touch Resistance Computation

To prevent bone penetration from a still (non-oscillating) saw, we also use the immersed information to calculate the force to prevent the penetration in haptic responses. The computation first transforms the device coordinates of the sample points (as the dot points in Fig. 3) on the saw surfaces into the volume coordinate as described in the above subsection. These sample points are in one voxel interval. Whether every sample point is inside a bone voxel is check. If it is, that means the saw has immersed (already touched) into the bone at this point. The resistance is than proportional to the number of the immersed points (inside the bone voxel). The direction of the touch resistance herein is set as the reverse of the saw movement direction to oppose against the saw moving into the bone and pushes back the saw to the bone surface.

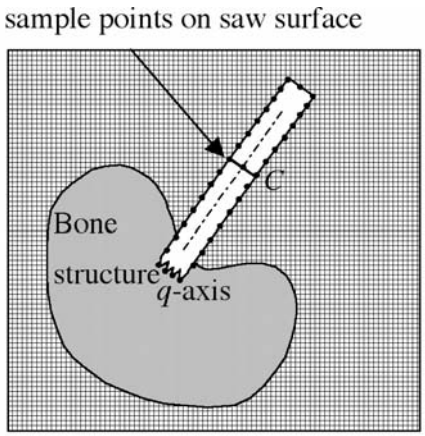

Fig. 3. Touch resistance computation.

2.4 Sawing Force Computation

This system calculates the load on the saw teeth to obtain the sawing force as the method described in the machining theorem [21-23]. In our model, every saw tooth is judged as cutting the bone if inside any bone voxel (as A illustrated in Fig. 4). That means the position of every tooth is transformed into the volume coordinate to check if in any bone voxel. If it is, this tooth is in sawing. The system then calculates the load for removing the bone chip on the tooth to sum up the sawing force.

For example, the area A^i of the i-th tooth (represented by the point at the tooth tip as T in Fig. 4) is calculated as $\triangle \times w \times p \times f/u$. $\triangle$ is 1 if this tooth is inside a bone voxel (i.e., in sawing), otherwise it is 0. w is the width of tooth blade. p, the tooth pitch, is the distance between any two teeth and can be considered constant. u is the frequency of the of the saw

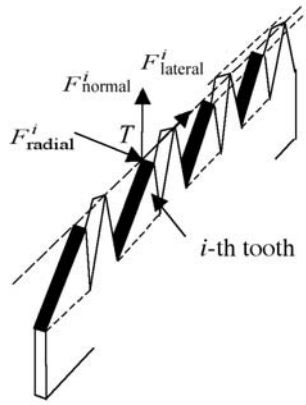

Fig. 4. Sawing force computation.

oscillation. The load acting on the i-th tooth can be represented as three following components as illustrated in Fig. 4,

$$F^i_{\text{lateral}} = K_{\text{lateral}} A^i \ , \quad F^i_{\text{radial}} = K_{\text{radial}} A^i \ , \quad F^i_{\text{normal}} = K_{\text{normal}} A^i$$

F_{normal}, the normal cutting force acts along the sawing direction. F_{radial}, the radial force is radial to the tooth face. F_{lateral}, The lateral force acts along the oscillating direction. F_x, F_y and F_z are the forces rendered to the x-, y- and z- axes (as illustrated in Fig. 2(C)) of the haptic device. F_y is equal to $\sum_i F^i_{\text{radial}}$, meaning summated from F_{radial} of all the teeth. In actual, the neighboring saw teeth are designed as facing opposite sides (as illustrated in Fig. 4) to cancel the radial forces generated from the neighboring teeth. However, F_x and F_y are determined from F_{normal} and F_{lateral} of all the teeth using the following equations.

$$F_z = \sum (\cos\theta^i F_{\text{normal}} - \sin\theta^i F_{\text{lateral}}) .$$

$$F_x = \sum (\sin\theta^i F_{\text{lateral}} + \cos\theta^i F_{\text{normal}}) .$$

θ^i, representing the angle of the i-th tooth regarding to the t-axis, is determined by the method described in Subsection 2.2. Because the saw oscillates about the t-axis, θ^i changes and then F_x and F_z. are cyclic according to the oscillation frequency. Meanwhile, because the angles of the saw teeth are small, F_z, the force against the saw feeding, is composed most of the normal forces and part of lateral forces acting the saw teeth. Similarly, F_x, the force against the oscillation, is composed most of the lateral forces and part of normal forces. F_y, the force pushing the saw sideways, is composed from the radial forces

acting on the saw teeth. The force coefficients $K_{lateral}$, K_{radial} and K_{normal} actually depend on many variables such as the saw rake angle, point angle, helix angle, cutting velocity and feed rate, the bone type (cancellous or cortical) etc, herein are set as constants and determined empirically corresponding to the types of saws and bones. Therefore, the sawing forces herein are linearly proportional to the feed rate and the inverse of the oscillation frequency for a specific saw and bone type.

3. IMPLEMENTATION

Any series of CT sections following the DICOM protocol can be the source data of our system. In the following, a patient with a typical amputation of extremity (distal femur) treated at the Orthopedic Department of Taipei Medical University Hospital in July 2005 was used to demonstrate the results implemented by our system. This 80-year-old man suffered from diabetes mellitus (D.M.) with repeated D.M. foot of the right low leg (sepsis with discharge sinus). He also had an osteoid osteoma over the right distal femur. After angiography and further orthosis planning distal femur amputation of extremity was performed. CT was performed in 94 transverse sections with 3mm intervals. Fig. 5 shows some results during the amputation surgery simulation. Fig. 5(A) shows a 3D image that reveals a tumor at the distal femur and a saw cutting the femur. Meanwhile, a hand piece equipped with a saw is used to cut the femur for separating the distal femur. The user separated the femur by four cuts. At each cut, the saw with ten teeth is fed perpendicular to the femur axis from the medial (inner) side to the lateral (outer) side and deeper inside the femur. Fig. 5(B) and Fig. 5(C) show that the separate patella, and then the distal femur and tibia have been removed to complete the amputation surgery.

Fig. 6 illustrates the calculated force F_x, F_y, F_z during the first cut. The user temped to keep the same feed speed and the oscillation speed is set as the same during the sawing process. F_x, F_y and F_z were rendered as the forces along the three primary axes of the haptic device, therefore were the forces the user felt. As shown in Fig. 6(A) and Fig. 6(B), F_z and F_x were cyclic with the saw oscillation frequency. F_z, mainly constituted from the normal forces of the saw teeth, therefore acts along the saw attitude direction. F_x, mainly constituted from the lateral forces of the saw teeth, therefore acts against the saw oscillation direction and vibrates as the saw oscillates. As shown in the two figures, the load of this cut increases because the depth immersed into the bone surface become larger and larger as the saw moved outward. However, when the forces are large and vibrate abruptly it became not easy to handle the hand piece. Therefore, the hand piece was pushed away to become uncut at several instants. In real bone sawing, such case usually occurs especially for inexperienced interns. F_y, constituted from the radial forces of the

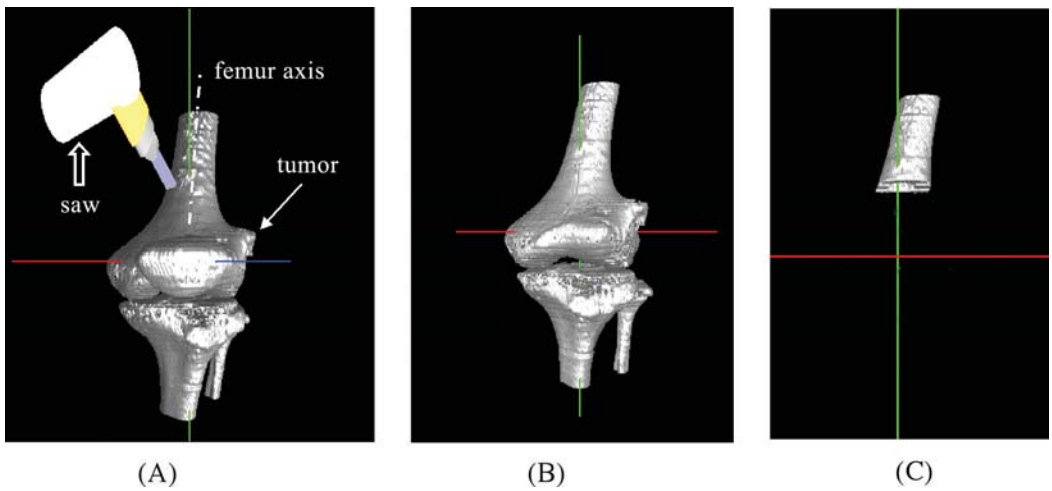

Fig. 5. Surgical simulations with haptic environment. Oblique view.
(A) A knee with a tumor at the femur. Gray area: reconstructed bone surface. Solid arrow: tumor on the femur. Hallow arrow: oscillating saw cutting the femur.
(B) The knee without the patella (that has already removed).
(C) The femur after amputation surgery. The distal femur and the tibia have already removed.

saw teeth, is small during the whole cut because most of the radial forces generated from the neighboring teeth cancel to each other. Because the feed rate is kept nearly the same, the remained radial force from one and sometimes two teeth has nearly the same value as shown in Fig. 6(C).

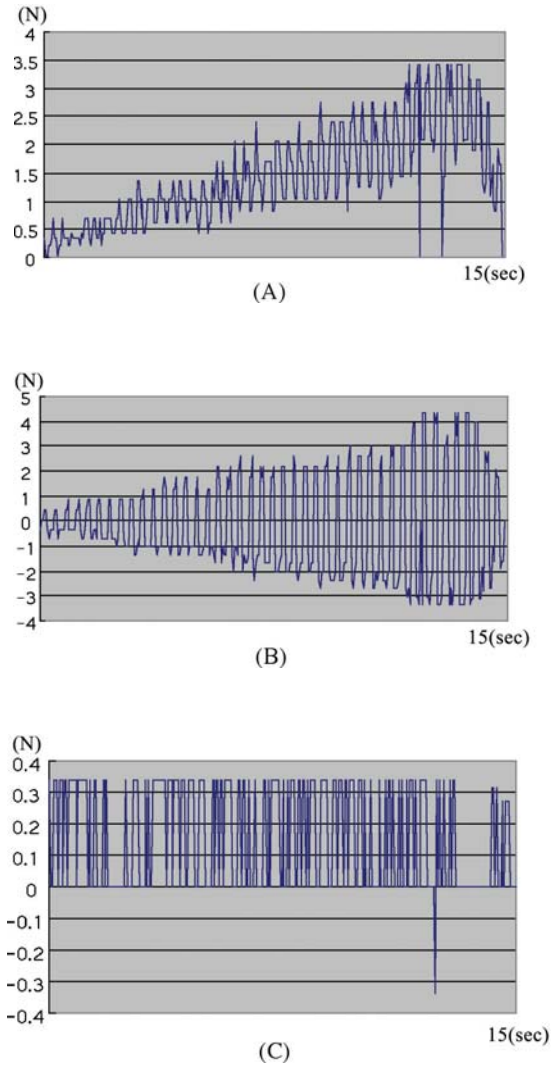

Fig. 6. Sawing forces from the saw entering and leaving the cortical bone.
(A) Force along the z-axis (saw attitude or normal direction) of the haptic device.
(B) Force along the x-axis (device attitude or oscillating direction) of the haptic device.
(C) Force along the y-axis (radial direction) of the haptic device.

4. DISCUSSION

The sawing resistances in orthopedic surgery usually violently oscillate to let the surgeon difficultly feed the saw and grasp the hand-piece, thus bring unstable sawing interface to lead bad healing. In this study, we have added haptic functions to precisely simulate the sawing process to our orthopedic surgical simulator so that not only geometric changes but also tactile bone sawing feeling can be provided for the amputation surgery simulations. The combination of the sawing haptic functions into our geometric surgery simulator that has been developed for visual verification, diagnoses and surgical planning provides a use of training interns and students with both tactile and visual interaction.

The proposed sawing force mode, modified from the metal sawing theorem, calculates the normal, lateral and radial forces on every tooth and then sums up these forces into the 3 positional forces for rendering the haptic device. Although the simulated forces provide the tactile feeling that resembles the real sawing, the force coefficients in our models are simplified to neglect the effects of the saw rake angle, point angle, helix angle, cutting velocity and feed rate. To achieve higher predicted accuracy, these coefficients should be studied to vary according to given specification (including age, sex, race and so forth) under statistically meaningful number of cases.

Other procedures in the amputation surgery such as soft tissue incision and suture should be realized into the haptic interaction simulator. Some suturing simulator provides haptic interaction but no geometric changes or deformations during surgery [24]. Our future work focuses on implementing these incision and suture procedures with both haptic and geometric responses. Therefore, the combination of the sawing haptic functions into our geometric surgery simulator provides successful simulations with both tactile and visual interaction.

5. CONCLUSION

Surgical simulation system allows surgeons to experience surgical procedures and haptic interfaces, thus to enable perception and delicate tactile sensations required in surgery. Therefore, combination of the sawing haptic functions into the orthopedic surgical simulator for training amputation surgery is important and has not yet developed until now. The proposed system manipulates the volume data of any specific patient to simulate the changes of bone geometry during amputation surgery and then uses the force computation models to simulate the haptic responses in

the sawing process based on the manipulated volume data.

Our force computation models calculate and then sum up the loads on saw teeth to obtain three positional forces that are used to render the haptic device and provide the user tactile environment for the amputation surgery. A simulation example demonstrates that changes of bone geometry can simulate the amputation geometry. Meanwhile, the simulated forces resemble the ones in the real sawing process and thus show the effectiveness of the sawing force computation models. Therefore, the combination of the haptic functions into our surgical simulator that has been developed for visual verification, diagnoses and surgical planning provides a use of training interns and students with both tactile and visual interaction.

ACKNOWLEDGMENT

This study was partially sponsored by the National Science Council (NSC), Taiwan/ROC; grant numbers NSC 94-2213-E-033-028, NSC 95-2213-E-033-065.

REFERENCE

1. Hsieh MS, Tsai MD, Yeh YD and Jou SB: Automatic spinal fracture diagnosis and surgical management based on 3D image analysis and reconstruction of CT transverse sections. Biomed. Eng Appl Basis Comm 2002; 14(5): 204-214.
2. Tsai MD, Yeh YD, Hsieh MS and Tsai CH: Automatic spinal disease diagnoses assisted by 3D unaligned transverse CT Slices. Comput Med Imag Graph 2004; 28(6): 307-319.
3. Tsai MD, Hsieh MS and Jou SB: Virtual reality orthopedic surgery simulator. Comput Biol Med 2001; 31(5): 333-351
4. Hsieh MS, Tsai MD and Yeh YD, Three-dimensional hip morphology analysis using CT transverse sections to automate diagnoses and surgery managements. Comput Biol Med 2005; 35(4): 347-371.
5. Hsieh MS, Tsai MD and Chung WC: Virtual reality simulator for osteotomy and fusion involving the musculoskeletal system. Comput Med Imag Grap. 2002; 26(2): 91-101.
6. Heng PA, Cheng CY, Wong TT, Xu , Chui YP, Chan KM and Tso SK: A virtual-reality training system for knee arthroscopic surgery. IEEE Trans Inform Technol Biomed 2004; 8(2): 217-227.
7. Xia J, Ip H, Samman N, Wong H, J. Gateno J, Wang D, Yeung R, Kot C and Tideman H: Three-dimensional virtual- reality surgical planning and soft-tissue prediction for orthognathic surgery. IEEE Trans Inform Technol Biomed 2001; 5(2): 97-107.
8. Lee TY, Lin CH and Lin HY: Computer-aided prototype system for nose surgery. IEEE Trans Inform Technol Biomed 2001; 5(4): 271-278.
9. Tsai MD, Chung WC and Hsieh MS: Three-dimensional landmarking based maxillomandibular deformity diagnosis using three-dimensional computer tomography. J Med Bio Eng 2002; 22(3): 129-13.
10. Monserrat C, Meier U, Alcañiz M, Chinesta F. and Juan MC: A new approach for the real-time simulation of tissue deformations in surgery simulation. Comput. Methods Programs Biomed 2001; 64: 77-85.
11. Kühnapfel U, Çakmak HK and Maaβ H: Endoscopic surgery training using virtual reality and deformable tissue simulation. Computer & Graphics 2000; 24: 671-682.
12. Choi KS, Sun H and Hen PA: Interactive deformation of soft tissues with haptic feedback for medical learning. IEEE Trans Inform Technol Biomed 2003; 7: 358-363.
13. Lee TY, Lin CH and Lin HY: Realistic rendering of an organ surface in real-time for laparoscopic surgery simulation. The Visual Computer 2002; 18: 135-149.
14. Cotin S, Delingette H and Ayache N: A hybrid elastic model for real-time cutting, deformations, and force feedback for surgery training and simulation. The Visual Computer 2000; 16: 437-452.
15. Agus M, Giachetti A, Gobbetti E, Zanetti G and Zorcolo A: Adaptive techniques for real-time haptic and visual simulation of bone dissection. IEEE Virtual Reality, IEEE CS press, 2003; 102-109.
16. Wang D, Zhang Y, Wang Y, Lee YS, Lu P, and Wang Y: Cutting on triangle mesh: local model-based haptic display for dental preparation surgery simulation. IEEE Trans on Visualization and Computer Graphics 2005; 11: 671-683.
17. Plaskos C, Hodgson AJ, Inkpen KB and McGraw RW: Bone-cutting errors in total knee arthroplasty. Journal of Arthroplasty 2002; 17(6): 698-705.
18. McCrea PH, Eng JJ and Hodgson AJ: Biomechanics of reaching: Clinical implications for individuals with acquired brain injury. Disability and Rehabilitation 2002; 24(10): 534-541.
19. Tsai MD and Hsieh MS: Volume manipulations for simulating bone and joint surgery. IEEE Trans Inform Technol Biomed 2005; 9(1): 139-149.
20. Lorensen WE and Cline HE: Marching Cubes: A high resolution 3D surface construction algorithm.

ACM SIGGraph Computer Graphics, Addision Wesley press, 1987; 163-169.
21. Ko TJ and Kim HS: Mechanistic cutting force model in band sawing. International Journal of Machine Tools & Manufacture 1999; 39: 1185-1197.
22. Henderer WE, Boor JD, Holston JR: Estimation of cutting forces in band sawing metals. Trans of NAMRC 1996; 24: 33-38.
23. Chandrasekaran H, Thoors H, Hellbergh H and Johansson L: Tooth chipping during band sawing of steel, Annals of the CIRP 1992; 41: 107-111.
24. O' Toole RV, Playter RR, Krummel TM, Blank WC, Cornelius NH, Roberts WR, Bell WJ, Raibert W: Measuring and developing suturing technique with a virtual reality surgical simulator, J Am Coll Surg 1999; 189(1): 114-127.